FULL PAPER

Pressure and temperature effects on metal-to-metal charge transfer in cyano-bridged Co^{III}–Fe^{II} complexes

Brendan P. Macpherson,*†[a] Basam M. Alzoubi,[b] Paul V. Bernhardt,[a] Manuel Martínez,[c] Peter A. Tregloan*[d] and Rudi van Eldik*‡[b]

[a] *Department of Chemistry, The University of Queensland, Brisbane, 4072, Australia*

[b] *Institute for Inorganic Chemistry, University of Erlangen-Nürnberg, Egerlandstr. 1, D-91058, Erlangen, Germany*

[c] *Departament de Química Inorgànica, Universitat de Barcelona, Martí i Franquès 1-11, E-08028, Barcelona, Spain*

[d] *School of Chemistry, The University of Melbourne, Parkville, 3052, Australia*

The effects of pressure and temperature on the energy (E_{op}) of the metal-to-metal charge transfer (MMCT, Fe^{II}→Co^{III}) transition of the cyano-bridged complexes *trans*-[L^{14}CoNCFe(CN)$_5$]$^-$ and *cis*-[L^{14}CoNCFe(CN)$_5$]$^-$ (where L^{14} = 6-methyl-1,4,8,11-tetraazacyclotetradecan-6-amine) were examined. The changes in the redox potentials of the cobalt and iron metal centres with pressure and temperature were also examined and the results interpreted with Marcus–Hush theory. The observed redox reaction volumes can mainly be accounted for in terms of localised electrostriction effects. The shifts in E_{op} due to both pressure and temperature were found to be less than the shifts in the energy difference ($\Delta E°$) between the Co^{III}–Fe^{II} and Co^{II}–Fe^{III} redox isomers. The pressure and temperature dependence of the reorganisational energy, as well as contributions arising from the different spin states of Co^{II}, are discussed in order to account for this trend. To study the effect of pressure on Co^{III} electronic absorption bands, a new cyano-bridged complex, *trans*-[L^{14}CoNCCo(CN)$_5$], was prepared and characterised spectroscopically and structurally. X-Ray crystallography revealed this complex to be isostructural with *trans*-[L^{14}CoNCFe(CN)$_5$]·5H$_2$O.

Introduction

Dinuclear complexes containing metal centres with variable oxidation states are of interest from a practical and theoretical standpoint particularly when metal-to-metal charge transfer (MMCT) transitions are present.[1–5] With a suitable choice of ligands and metal centres, these MMCT transitions fall in the visible region, opening up the possibility of reversible electrochromism by switching this transition through oxidation or reduction of one of the metal centres. The energy of the optical electron transfer transition (E_{op}) is related to the energy difference between the thermally equilibrated ground and excited states ($\Delta G°$) and the reorganisational energy λ by the expression[3–7]

$$E_{op} = \Delta G° + \lambda \qquad (1)$$

$\Delta G°$ can usually be approximated as the difference in the redox potentials of the donor and acceptor metal centres $-nF\Delta E°$ (where $n = 1$ for an MMCT process), and thus it follows from eqn. (1), that tuning of the MMCT transition energy may be achieved by making modifications to the complex that alter the redox potentials of the metal centres involved. Our recent investigations of a series of complexes of the type [LCoNCM(CN)$_5$]$^-$ (where L is a pentaamine or triaminedithiaether macrocyclic ligand and M = Fe^{II} or Ru^{II}) have illustrated this principle. We found that changing the size of the macrocyclic ring and its geometry of binding produced small variations in the MMCT energy, whereas larger shifts were observed upon changing the donor set of the macrocycle (from N$_5$ to N$_3$S$_2$) or the MMCT donor metal unit.[8–12] A good correlation of the MMCT energies of these complexes with $\Delta G°$ was found within the experimental uncertainties involved; the correlation with changes to λ are less pronounced.

Having achieved tuning of the MMCT through structural changes, we turn now to investigate the influence of external parameters, namely pressure and temperature, on the MMCT energy and redox potentials of the complexes. Pressure and temperature are known to have considerable effects on the redox potentials of metal complexes,[13–21] and hence we were interested to see the influence that the pressure and temperature induced redox tuning had on the spectra of these complexes.

The application of high-pressure techniques is also able to yield useful information about reaction and activation volumes of chemical reactions.[16,22,23] For electron-transfer reactions, the cell reaction volume may be obtained by measuring the change in the redox potential with pressure, at constant temperature, according to the relationship given in eqn. (2).

$$\Delta V = -nF\left(\frac{\partial E°}{\partial P}\right)_T \qquad (2)$$

The observed reaction volume corresponds to the sum of the volume contributions of the reference and complex half-reactions (eqns. (3) and (4)).

$$\text{complex}^{z+} + \text{ref} \longrightarrow \text{complex}^{(z-1)+} + \text{ref}^+ \qquad (3)$$
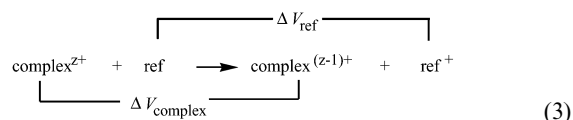
$$\Delta V_{cell} = \Delta V_{ref} + \Delta V_{complex} \qquad (4)$$

By using a reference half-cell with known reaction volume, the redox reaction volume of the complex under investigation can be calculated. This volume change, $\Delta V_{complex}$, is made up of intrinsic (inner sphere) and electrostrictive (outer sphere) volume changes (eqn. (5)).

$$\Delta V_{complex} = \Delta V_{intr} + \Delta V_{electr} \qquad (5)$$

If the redox reaction volumes for oxidation and reduction of the donor and acceptor moieties in a mixed valence complex are significant, it will be possible to alter the redox isomer energy

difference of the complex by applying pressure, which will in turn affect the energy of the MMCT transition. MMCT transitions in highly localised (Robin and Day Class II)[1] mixed valence complexes are also known to be affected by temperature.[20,21,24–26] This is mainly due to the temperature dependence of the redox potentials of the metal centres involved in the transition, which changes the energy difference ($\Delta G°$) between the ground and excited states.

In this work, we present the influence of pressure and temperature on the spectroscopy and electrochemistry of *trans*- and *cis*-[L^{14}CoNCFe(CN)$_5$]$^-$ (L^{14} = 6-methyl-1,4,8,11-tetraazacyclotetradecan-6-amine, see Chart 1). The redox reaction volumes of the complexes are evaluated in terms of the contributions from intrinsic and electrostrictive components and the influence of the cyano-bridge on the effective charge at the metal centres is discussed. The results are correlated with the effect of pressure and temperature on the energy (E_{op}) of the MMCT transition of the cyano-bridged complexes. Possible complications arising from different spin states of Co^{II} are discussed.
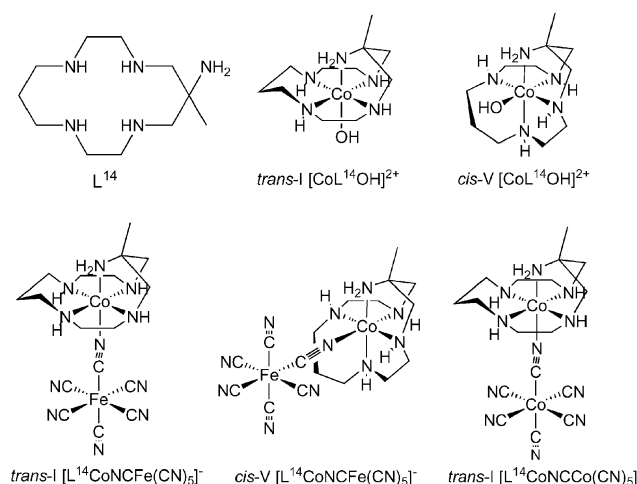

Chart 1

Experimental

Syntheses

A solution of *cis*-[CoL^{14}(OH)]$^{2+}$ was prepared by base hydrolysis of *cis*-[CoL^{14}Cl]Cl$_2$, which was prepared essentially as previously described.[27] A suitable amount was dissolved in 0.1 M NaClO$_4$ and 0.1 M NaOH solution was added to pH 11. Rapid hydrolysis of the complex was observed by means of UV/vis spectroscopy and cyclic voltammetry. A solution of *trans*-[CoL^{14}(OH)]$^{2+}$ (the more stable geometric isomer) was prepared *in situ* from *cis*-[CoL^{14}(OH)]$^{2+}$ by heating the above solution at *ca.* 60 °C for 30 min at pH 12. Complete isomerisation was confirmed by UV/vis spectroscopy and cyclic voltammetry. *trans*-Na[L^{14}CoNCFe(CN)$_5$] was prepared as previously described.[9] All other reagents were obtained commercially.

***cis*-Na[L^{14}CoNCFe(CN)$_5$].** This has been reported previously,[10] but here was prepared *in situ* by heating a mixture of *cis*-[CoL^{14}Cl]$^{2+}$ and [Fe(CN)$_6$]$^{4-}$ at *ca.* 60 °C until the solution had darkened in colour. The formation of the dinuclear complex was confirmed by the appearance of the typical Fe$^{III/II}$ wave *ca.* 200 mV more positive of the ferri/ferrocyanide wave in the cyclic voltammogram and the optical spectrum was also identical to that reported.[10]

***trans*-[L^{14}CoNCCo(CN)$_5$]·5H$_2$O.** *trans*-[CoL^{14}Cl](ClO$_4$)$_2$ (0.26 g; 0.5 mmol) was dissolved in 200 mL water, the pH adjusted to *ca.* 8 with 0.1 M NaOH and the solution stirred for 10 min to allow hydrolysis of the complex. The pH was then

lowered to *ca.* 5 with 0.1 M HCl, and then K$_3$[Co(CN)$_6$] (0.17 g; 0.5 mmol) in *ca.* 20 mL water was added. The solution was stirred at *ca.* 60 °C overnight, after which the pH was measured to be *ca.* 8.5. Dilute HCl was added (*ca.* pH 6), and stirring was continued for a further 5 h. The solution was then left to stand at room temperature, upon which small yellow crystals formed, which were suitable for X-ray crystallography (0.07 g, 24%). Anal. Calc. for C$_{17}$H$_{37}$Co$_2$N$_{11}$O$_5$: C, 34.41; H, 6.28; N, 25.96%. Found: C, 34.24; H, 6.14; N, 25.94%. Electronic spectral data (H$_2$O), λ_{max}/nm (ε/M^{-1} cm^{-1}): 451 (104), 315 (347). ^{1}H NMR (D$_2$O, TSP): δ 1.33 (s, –CH$_3$), 2.3–3.8 ppm (m, –CH$_2$–). IR (KBr disk) $\tilde{\nu}$/cm^{-1}: 2134 (s, equatorial CN), 2151 (m, axial CN), 2179 (m, μ-CN).

Electrochemistry

The experimental set-up for high-pressure electrochemistry has been previously described.[16] A 2-mm diameter glassy carbon electrode was employed for the working electrode and 2 mm platinum electrodes were used for the auxiliary and pseudo-reference electrodes. A MacLab potentiostat and software (AD Instruments Pty Ltd) were used to record the cyclic voltammograms. Potassium ferrocyanide was added to the solutions under investigation to act as an internal reference since the molar volume change of ferrocyanide upon reduction has been previously studied.[14–16] Solutions were made up in 0.1 M NaClO$_4$ electrolyte with *ca.* 3 mM concentrations of complex, and *ca.* 2 mM potassium ferrocyanide. Ideally, temperature-dependent electrochemistry should be carried out using a non-isothermal cell configuration in order to avoid errors introduced by the temperature dependence of the reference half-cell.[18] However, since we were primarily interested in the difference between potentials rather than absolute values, the experimental setup was simplified by using an isothermal cell. Ferrocyanide was added as an internal standard, allowing estimation of absolute values based on the temperature dependence of its redox couple.[17] Temperature dependent electrochemistry was performed using a BAS100B/W potentiostat with a 3 mm diameter glassy-carbon working electrode, a platinum-wire auxiliary electrode, and a silver/silver chloride reference electrode, with the temperature of the electrochemical cell adjusted by means of a circulating water jacket. A scan rate of 100 mV s^{-1} was used in all experiments. The average of the anodic and cathodic peaks was measured, which equates to the redox potential ($E°$) assuming the diffusion coefficients of the oxidised and reduced forms of the couple are the same.[28] A typical cyclic voltammogram is shown in Fig. 1.
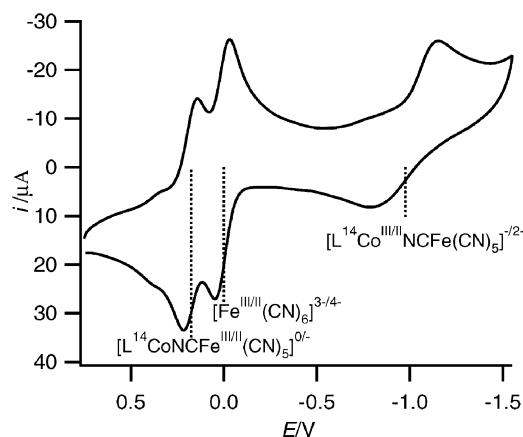
Fig. 1 Cyclic voltammogram at 138 MPa of *cis*-[L^{14}CoNCFe(CN)$_5$]$^-$ referenced to [Fe(CN)$_6$]$^{4-}$ internal reference.

Electronic spectroscopy

The high-pressure spectra were recorded on a Shimadzu UV-2101 spectrophotometer, employing a homemade cell holder and

pillbox cell as described previously.[29] Temperature dependent spectra were measured on a Perkin-Elmer Lambda 12 spectrophotometer, fitted with a Peltier temperature controller.

Crystallography

Cell constants were determined by a least-squares fit to the setting parameters of 25 independent reflections measured on an Enraf-Nonius CAD4 four-circle diffractometer employing graphite-monochromated Mo-Kα (0.71073 Å) radiation and operating in ω–2θ Å scan mode. Data reduction and empirical absorption corrections (ψ-scans) were performed with the WinGX package.[30] The structure was solved by direct methods with SHELXS-97 and refined by full-matrix least-squares analysis with SHELXL-97.[31] The molecular plot was produced with ORTEP.[32] All non-hydrogen atoms were modelled using anisotropic thermal parameters. Alkyl and amine H-atoms were fixed at calculated positions. Water H-atoms were located from the difference map and constrained to a riding model in subsequent refinement.

Crystal data. $C_{17}H_{37}Co_2N_{11}O_5$, $M = 593.44$, monoclinic, space group $P2_1/c$ (no. 14), $a = 9.9425(6)$, $b = 13.294(2)$, $c = 20.143(2)$ Å, $\beta = 90.66(1)°$, $U = 2262.2(5)$ Å^3, $T = 293$ K, $Z = 4$, μ(Mo-Kα) $= 1.295$ mm^{-1}, 4962 reflections measured, 4676 unique ($R_{int} = 0.0502$), $R_1 = 0.0391$, $wR_2 = 0.1043$ (all data).

CCDC reference number 263590.

See http://www.rsc.org/suppdata/dt/b4/b418054b/ for crystallographic data in CIF or other electronic format.

## Results and discussion

trans-[L^{14}CoNCCo(CN)$_5$] complex

The crystal structure of the trans-[L^{14}Co^{III}NCCo^{III}(CN)$_5$]·5H$_2$O complex reported herein (Fig. 2) is isostructural with the previously reported trans-[L^{14}Co^{III}NCFe^{III}(CN)$_5$]·5H$_2$O.[10] As expected, the Co–CN coordinate bond lengths are slightly shorter (by an average of 0.03 Å; Table 1) than those found in the ferricyanide relative, and correlate with a slightly smaller unit cell in the present structure. These trends are also observed in the structures of K$_3$[Fe(CN)$_6$] and K$_3$[Co(CN)$_6$].[33] No other significant differences are observed between the two structures.

Two bands are observed in the UV-visible spectrum of trans-[L^{14}CoNCCo(CN)$_5$], shown in Fig. 3 along with the spectra of trans and cis-[L^{14}CoNCFe(CN)$_5$]$^-$. The lowest energy band at 451 nm ($\varepsilon = 104$ M^{-1} cm^{-1}) is assigned to the $^1T_{1g} \leftarrow {}^1A_{1g}$ transition of the macrocyclic cobalt centre, while the band observed at 315 nm ($\varepsilon = 347$ M^{-1} cm^{-1}) results from contributions from the $^1T_{1g} \leftarrow {}^1A_{1g}$ transition of cyano cobalt centre as well as the $^1T_{2g} \leftarrow {}^1A_{1g}$ transition of macrocyclic cobalt centre.[34]

The cyclic voltammograms of trans-[L^{14}CoNCCo(CN)$_5$] reveal single quasi-reversible Co$^{III/II}$ couples corresponding to the macrocyclic cobalt centre at -568 and -555 mV (vs. Ag/AgCl)
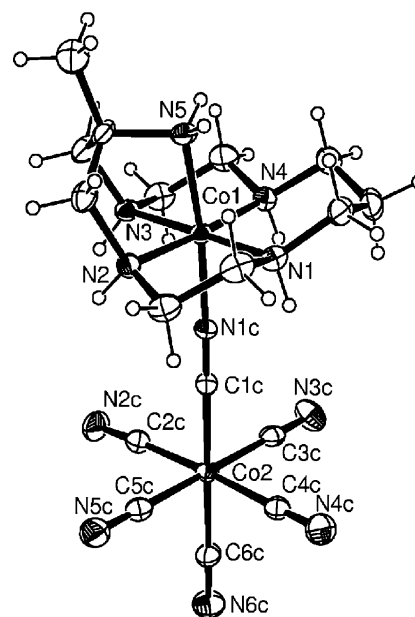
Fig. 2 ORTEP view of trans-[L^{14}CoNCCo(CN)$_5$] (30% probability ellipsoids).
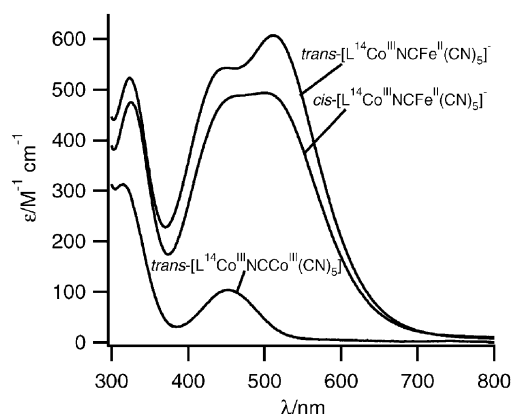
Fig. 3 Electronic spectra of trans-[L^{14}CoNCCo(CN)$_5$], trans-[L^{14}CoNCFe(CN)$_5$]$^-$ and cis-[L^{14}CoNCFe(CN)$_5$]$^-$.

on glassy carbon and dropping mercury working electrodes, respectively. The ca. 240 mV anodic shift of this couple with respect to the analogous hexacyanoferrate(II) complex (trans-[L^{14}Co$^{III/II}$NCFe(CN)$_5$]$^{-/2-}$) reveals the electrostatic influence of the trianionic hexacyanocobaltate(III) moiety as opposed to the tetraanionic ferrocyanide group. The Co$^{III/II}$ couple of the hexacyanocobaltate centre was not accessible within the potential window examined.

Table 1 Selected bond lengths (Å) of trans-[L^{14}CoNCCo(CN)$_5$]·5H$_2$O and trans-[L^{14}CoNCFe(CN)$_5$]·5H$_2$O

	trans-[L^{14}CoNCCo(CN)$_5$]·5H$_2$O	trans-[L^{14}CoNCFe(CN)$_5$]·5H$_2$O[a]
Co1–N1	1.956(4)	1.961(4)
Co1–N2	1.948(4)	1.95(4)
Co1–N3	1.953(4)	1.948(4)
Co1–N4	1.956(4)	1.962(4)
Co1–N5	1.943(4)	1.947(4)
Co1–N1C	1.909(4)	1.914(4)
M–C1C	1.903(5)	1.934(6)
M–C2C	1.892(6)	1.922(7)
M–C3C	1.907(6)	1.925(7)
M–C4C	1.900(6)	1.936(7)
M–C5C	1.895(6)	1.934(7)
M–C6C	1.890(5)	1.933(6)

[a] Ref 10.

Optical measurements

The pressure and temperature dependent UV-visible spectra of *trans* and *cis*–[L^{14}CoNCFe(CN)$_5$]$^-$ are shown in Figs. 4 and 5. The insets show the changes in the maxima of the MMCT bands, which display opposite trends with increasing pressure and temperature. With increasing pressure, the MMCT shifts to higher energy, with a slight decrease in band intensity, whereas with increasing temperature, the MMCT band shifts to lower energy and gains intensity.

The dependence of E_{op} on pressure ($\partial E_{op}/\partial P$) and temperature ($\partial E_{op}/\partial T$) determined from the gradient of these plots is indicated in Table 2. There is little difference between the values of $\partial E_{op}/\partial P$ and $\partial E_{op}/\partial T$ for the two isomers, which fall within the range of values for previously studied Ru^{III}–Fe^{II} and Ru^{III}–Ru^{II} complexes.[21,24–26,35]

Along with the decrease in the intensity of the MMCT band at *ca.* 500 nm with increasing pressure, the intensities of the bands assigned to the cobalt and iron $^1T_{1g} \leftarrow {}^1A_{1g}$ transitions at *ca.* 430 and 320 nm, respectively, were observed to increase. It was unsure whether these intensity changes were related, so in order to further examine the intensity changes of the d–d bands, the pressure dependent spectra of the isoelectronic Co^{III}–Co^{III} complex *trans*-[L^{14}CoNCCo(CN)$_5$]·5H$_2$O were measured. The spectra show negligible changes in the energy and intensity ($\Delta\tilde{v}_{max} < 50$ cm^{-1}, $\Delta\varepsilon \approx 3$ M^{-1} cm^{-1}) of the lower energy d–d electronic maximum (Co^{III}N$_6$, $^1T_{1g} \leftarrow {}^1A_{1g}$) over

a 150 MPa pressure range. This indicates that the pressure effects on the intensity of the d–d electronic maxima of *trans*- and *cis*-[L^{14}Co^{III}NCFe^{II}(CN)$_5$]$^-$ result from overlap with the MMCT band, which shifts to lower wavelength with increasing pressure. The intensities of the MMCT bands of *trans*- and *cis*-[L^{14}Co^{III}NCFe^{II}(CN)$_5$]$^-$ were found to increase with increasing temperature, while the d–d transition intensities showed minimal temperature dependence. This is opposite to the pressure effect.

Electrochemical measurements

The shift in the redox potentials (referenced to the ferro/ferricyanide internal reference) of the complexes *trans*- and *cis*-[L^{14}CoNCFe(CN)$_5$]$^-$ with pressure is shown in Fig. 6. The molar volume change for ferri/ferrocyanide reduction has been previously determined for a range of conditions.[14–16] The volume changes for the working electrode reaction ($\Delta V_{complex}$) were determined by subtracting ΔV_{ref} (29.8 cm^3 mol^{-1} for [Fe(CN)$_6$]$^{3-/4-}$ in 0.1 M KNO$_3$)[14] from the values of ΔV_{cell} derived from the pressure dependencies of the measured cell potentials (eqn. (4)). These results are collected in Table 3 and may be separated into contributions from intrinsic and electrostrictive effects.[14–16]

The electrostrictive volume change for spherical charges depends on ($\Delta z^2/r$), however, the estimation of effective radius for a metal complex is problematic[15] and it has recently been suggested[36] that apparent radii of some electro-active species
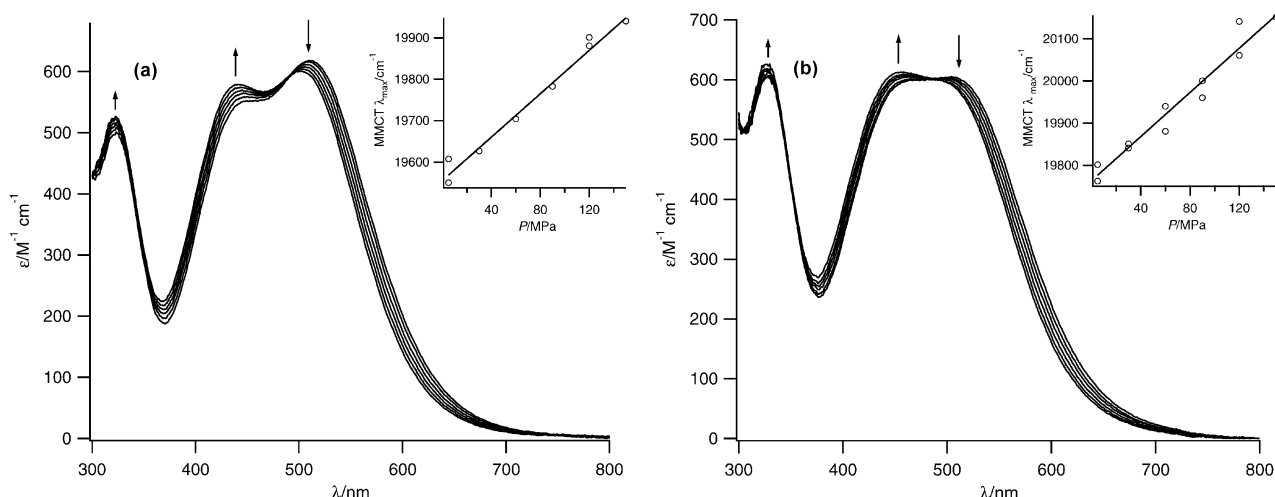
Fig. 4 Pressure dependence of the electronic spectra of (a) *trans*-[L^{14}CoNCFe(CN)$_5$]$^-$ and (b) *cis*-[L^{14}CoNCFe(CN)$_5$]$^-$. Arrows point in the direction of increasing pressure. Insets show pressure dependent energy changes of the respective MMCT band.
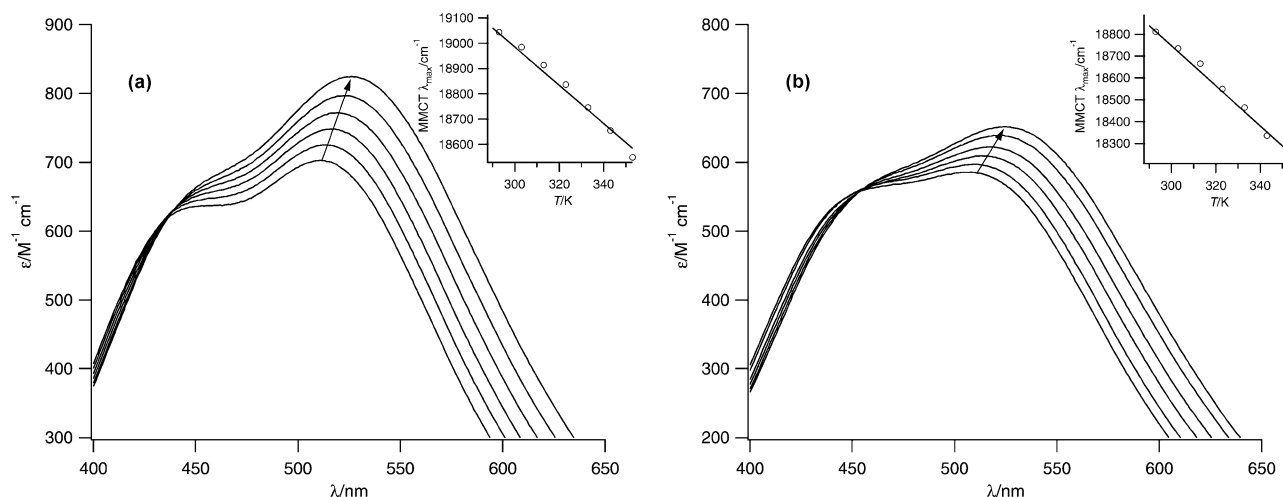

Fig. 5 Temperature dependent electronic spectra of (a) *trans*-[L^{14}CoNCFe(CN)$_5$]$^-$ and (b) of *cis*-[L^{14}CoNCFe(CN)$_5$]$^-$. Arrows point in the direction of increasing temperature. Insets show temperature dependence of the MMCT band maximum.

Table 2 Temperature and pressure dependence of E_{op} and ΔE°

Complex	$(\partial E_{op}/\partial T)/cm^{-1}\ K^{-1}$	$[\partial(\Delta E^\circ)/\partial T]/^a/cm^{-1}\ K^{-1}$	$(\partial E_{op}/\partial P)/cm^{-1}\ MPa^{-1}$	$[\partial(\Delta E^\circ)/\partial P]^a/cm^{-1}\ MPa^{-1}$
Asymmetric systems				
$trans$-$[L^{14}Co^{III}NCFe(CN)_5]^{-\ b}$	-10.2 ± 0.4	-16.8 ± 0.5	2.6 ± 0.1	3.2 ± 0.1
cis-$[L^{14}Co^{III}NCFe^{II}(CN)_5]^{-\ b}$	-12.4 ± 0.6	-18.1 ± 0.6	2.6 ± 0.5	3.9 ± 0.1
$[(NH_3)_5Ru^{III}NCFe^{II}(CN)_5]^{-\ c,d}$	-13.5 ± 1	-9.2 ± 1.5	3.00	2.72
$[(NH_3)_5Ru^{III}CNRu^{II}(CN)_5]^{-\ c}$	-13			
$[(edta)Ru^{III}NCFe^{II}(CN)_5]^{5-\ d,e}$	-5 ± 0.4	-6 ± 1	0.97	1.74
$[(edta)Ru^{III}NCRu^{II}(CN)_5]^{5-\ f}$	-4.1	-3.5		
$[(hedta)Ru^{III}NCFe^{II}(CN)_5]^{4-\ g}$	-6.8 ± 0.5	-6.2 ± 1.1		
$[(bpy)ClRu^{III}(pyrz)Ru^{II}(NH_3)_5]^{4+\ h}$	-18	-8		
Symmetric systems				
$[Fe(CN)_6]^{3-}; [Fe(CN)_6]^{4-\ i}$	2.9		-1.33	
$[(NH_3)_5Ru^{III}(S–S)Ru^{II}(NH_3)_5]^{5+\ j}$			-1.44	
$[(CN)_5Fe^{III}(4,4'\text{-bipy})Fe^{II}(CN)_5]^{5-\ c}$	0.1 ± 0.6			

^{a} Expressed in 'spectroscopic' units for comparison. ^{b} This work. ^{c} Ref 21. ^{d} Ref 26. ^{e} Ref 25. ^{f} Ref 41. ^{g} Ref 35. ^{h} Ref 24. ^{i} Ref 39. ^{j} Ref 40.
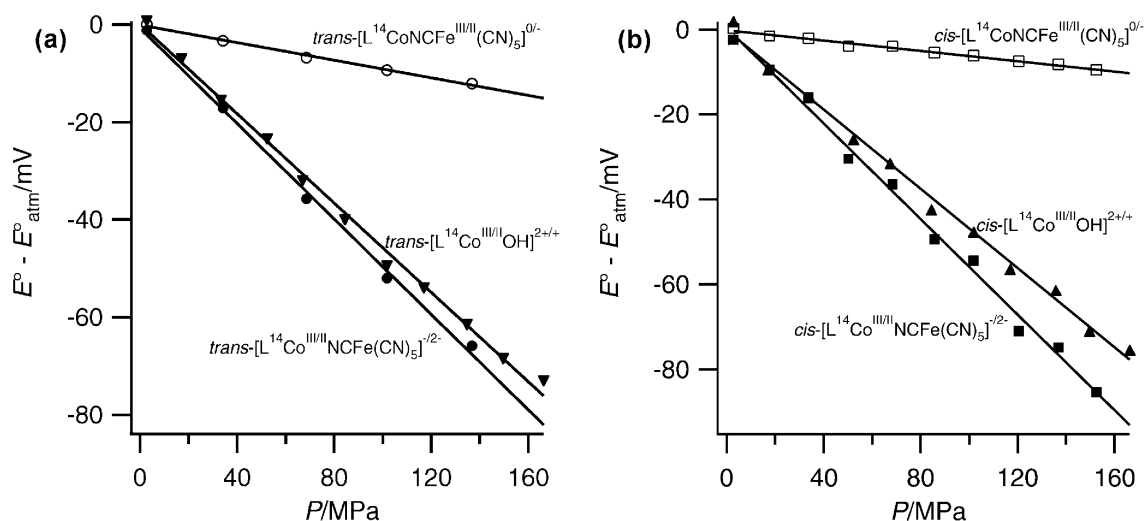
Fig. 6 Pressure dependent variations in the redox potentials of (a) (○) $trans$-$[L^{14}CoNCFe^{III/II}(CN)_5]^{0/-}$, (●) $trans$-$[L^{14}Co^{III/II}NCFe(CN)_5]^{-/2-}$, (▼) $trans$-$[L^{14}Co^{III/II}(OH)]^{2+/+}$; (b) (□) cis-$[L^{14}CoNCFe^{III/II}(CN)_5]^{0/-}$, (■) cis-$[L^{14}Co^{III/II}NCFe(CN)_5]^{-/2-}$, (▲) cis-$[L^{14}Co^{III/II}(OH)]^{2+/+}$. All potentials are relative to the $[Fe(CN)_6]^{3-/4-}$ internal standard.

in a range of non-aqueous solvents may be of little physical significance. So, given that the redox centres being reported here are of comparable size to those described previously, we have estimated ΔV_{electr} at ionic strengths around 0.1 M using the empirically developed eqn. (6) that has proved useful in similar situations.[15,37]

$$\Delta V_{electr} = 4.3\Delta z^2 \qquad (6)$$

In eqn. (6), Δz^2 is the difference between the squares of the charges of oxidised and reduced forms of the complex. For $[Fe(CN)_6]^{3-/4-}$, Δz^2 is -7 $((-3)^2 - (-4)^2)$, and using this equation, ΔV_{electr} was calculated as $-30.1\ cm^3\ mol^{-1}$ (Table 3). Using the experimentally determined reaction volume and eqn. (5) leads to $\Delta V_{intr} = 0.3\ cm^3\ mol^{-1}$ for the ferri/ferrocyanide couple, which is within experimental error of the expected value of 0.[33] Given the fact that the crystal structures of $trans$- and cis-$[L^{14}CoNCFe(CN)_5]^{-/0}$ (with Fe in oxidation states of II and III) show minimal differences (*ca.* 0.02 Å) in the Fe–C bond lengths,[9,10] the intrinsic reaction volume of the Fe$^{III/II}$ couple is expected to be negligible, and thus $\Delta V_{electr} \approx \Delta V_{complex}$. Using eqn. (6) and the experimental values collected in Table 3, the value of Δz^2 can be estimated to be -4.9 and -5.6 for $trans$- and cis-$[L^{14}CoNCFe(CN)_5]^-$, respectively. A value of -5 is

consistent with an effective $2-/3-$ charge change localised around the iron centre. Comparing this to ferri/ferrocyanide, this represents a shift in approximately one electronic charge from the iron centre through the bridging cyanide to the cobalt centre, which is in line with the *ca.* 150 mV anodic shift of the Fe$^{III/II}$ redox potential relative to free ferrocyanide. Similar shifts in potential ($\sim$200 mV) and implied effective charges ($2-/3-$) have also been reported in $[(NH_3)_5RuNCFe(CN)_5]^{0/-}$ and $[(EDTA)RuNCFe(CN)_5]^{4-/5-}$.[37]

For $trans$- and cis-$[L^{14}Co(OH)]^{2+/+}$, Δz^2 is $+3$, producing a ΔV_{electr} of 12.9 cm^3 mol^{-1}. From the experimentally determined reaction volumes (Table 3), this value leads to ΔV_{intr} of $+2.0$ and $+8.3\ cm^3\ mol^{-1}$ for the *trans* and *cis* isomers, respectively. If we assume that the values of ΔV_{intr} for the Co$^{III/II}$ couples of both the dinuclear ($[L^{14}CoNCFe(CN)_5]^-$) and mononuclear ($[CoL^{14}(OH)]^{2+}$) complexes are the same (*i.e.* the coordinated ferrocyanide does not influence internal variations in the Co–N bond lengths), which is consistent with available structural data,[9,10] the back-calculated value of ΔV_{electr} is similar for the two isomers of $[L^{14}CoNCFe(CN)_5]^-$ (Table 3). This produces an estimated value of Δz^2 that corresponds to a change in effective charge of $2+/+$ upon reduction of the Co^{III} centre for the dinuclear complexes. The cobalt centres in the dinuclear complexes gain a negative charge from the bridging cyanide,

Table 3 Values of reduction potentials and reaction volumes determined in this study

Complex	$E°^a$/mV	ΔV_{cell}/cm³ mol⁻¹	$\Delta V_{complex}$/cm³ mol⁻¹	$z_1/z_2{}^b$	Δz^b	$\Delta V_{electr}{}^b$/cm³ mol⁻¹	$\Delta V_{intr}{}^b$/cm³ mol⁻¹
[Fe$^{III/II}$(CN)$_6$]$^{3-/4-}$ (reference)	0	0	−29.8	3−/4−	→ −7.0	→ −30.1	→ 0.3
trans-[L^{14}Co$^{II/I}$(OH)]$^{2+/+}$	−967	44.7 ± 1.6	14.9	2+/+	→ 3.0	→ 12.9	→ 2.0
cis-[L^{14}Co$^{II/I}$(OH)]$^{2+/+}$	−881	51.0 ± 2.4	21.2	2+/+	→ 3.0	→ 12.9	→ 8.3
trans-[L^{14}Co$^{III/II}$NCFe$^{III/II}$(CN)$_5$]$^{0/-}$	217	8.8 ± 0.2	−21.0	~2−/3−	−4.9 ↓	−21.0 ↓	0.0 ↓
cis-[L^{14}Co^{III}NCFe$^{III/II}$(CN)$_5$]$^{0/-}$	179	5.9 ± 0.4	−23.9	~2−/3−	−5.6 ↓	−23.9 ↓	0.0 ↓
trans-[L^{14}Co$^{III/II}$NCFe^{II}(CN)$_5$]$^{-/2-}$	−975	47.3 ± 1.1	17.5	~2+/+	3.6 ↓	15.5 ↓	2.0 ↓
cis-[L^{14}Co$^{III/II}$NCFe^{II}(CN)$_5$]$^{-/2-}$	−908	53.1 ± 1.9	23.3	~2+/+	3.5 ↓	15.0 ↓	8.3 ↓

^{a} Referenced to [Fe(CN)$_6$]$^{3-/4-}$. ^{b} The arrows show the flow of the argument in deriving values. See text for details.
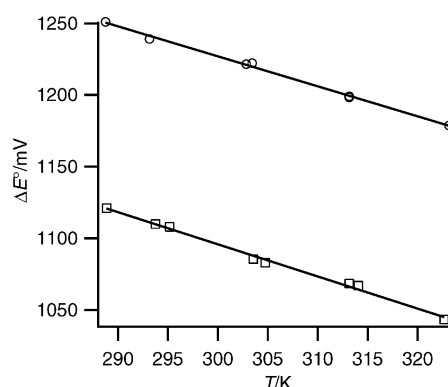
which is complementary to the effects indicated above on the iron centre of these complexes.

The intrinsic volume changes at the cobalt centres in this study are less than those for other complexes with non-macrocyclic ligands, such as [Co(en)$_3$]$^{3+/2+}$ and [Co(phen)$_3$]$^{3+/2+}$, but similar to those in the cage complexes [Co(sep)]$^{3+/2+}$ and [Co(diamsar)]$^{3+/2+}$.[16] The trend in the values for the cis and trans isomers (ΔV_{intr}(cis) > ΔV_{intr}(trans)) is in agreement with molecular mechanics modelling calculations,[10] which predicted a greater increase in Co–N bond lengths for the cis isomer upon reduction. The cis coordinated macrocycle, with its folded conformation, is better able to accommodate expansion of the cobalt ion upon reduction than the trans configuration, where the macrocycle encircles the metal and more effectively restricts coordinate bond expansion. This effect was seen previously during a study of the outer-sphere reduction of the isomeric cis- and trans-[CoL^{14}(H$_2$O)]$^{3+}$ complexes.[38]

The redox isomer energy difference ($\Delta E°$), measured from the difference between the redox potentials of the Co$^{III/II}$ and Fe$^{III/II}$ redox couples, decreases with temperature for both trans- and cis-[L^{14}CoNCFe(CN)$_5$]$^-$, as shown in Fig. 7. Table 2 shows a comparison of the dependence on temperature and pressure of the redox isomer energy difference (converted to units of cm^{-1}) and the MMCT energy. From the temperature dependence of the energy difference between the redox isomers, the entropy change ΔS_{et} accompanying the thermally activated electron transfer reaction (eqn. (7)) may be evaluated (eqn. (8)).
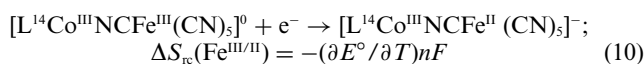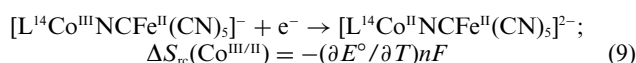
$$[L^{14}Co^{III}NCFe^{II}(CN)_5]^- \rightarrow [L^{14}Co^{II}NCFe^{III}(CN)_5]^- \qquad (7)$$
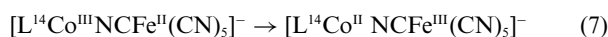
$$\Delta S_{et} = -nF\left(\frac{\partial(\Delta E°)}{\partial T}\right)_P \qquad (8)$$

Fig. 7 Temperature dependence of $\Delta E°$ ($E°_{Co} - E°_{Fe}$) for (○) trans-[L^{14}CoNCFe(CN)$_5$]$^-$ and (□) cis-[L^{14}CoNCFe(CN)$_5$]$^-$.

The reaction entropies (ΔS_{et}) obtained in this way (Fig. 7) are 202 ± 5 and 216 ± 7 J K^{-1} mol^{-1} for the trans- and cis-[L^{14}CoNCFe(CN)$_5$]$^-$ complexes, respectively.

The redox entropies of the individual metals centres may also be calculated by taking into account the contribution of the reference couple to the observed change in cell potential ($\partial E°/\partial T = -2.69$ mV K^{-1} for the [Fe(CN)$_6$]$^{3-/4-}$ internal reference).[17] Values for the redox entropies ΔS_{rc} of −21 ± 6 and −24 ± 25 J K^{-1} mol^{-1} for the Co$^{III/II}$ couples of the trans and cis isomers of [L^{14}Co^{III}NCFe^{II}(CN)$_5$]$^-$, respectively (eqn. (9)), and −222 ± 2 and −240 ± 28 J K^{-1} mol^{-1} for the Fe$^{III/II}$ couples of the trans and cis isomers (eqn. (10)), respectively, are obtained.

$$[L^{14}Co^{III}NCFe^{II}(CN)_5]^- + e^- \rightarrow [L^{14}Co^{II}NCFe^{II}(CN)_5]^{2-};$$
$$\Delta S_{rc}(Co^{III/II}) = -(\partial E°/\partial T)nF \qquad (9)$$

$$[L^{14}Co^{III}NCFe^{III}(CN)_5]^0 + e^- \rightarrow [L^{14}Co^{III}NCFe^{II}(CN)_5]^-;$$
$$\Delta S_{rc}(Fe^{III/II}) = -(\partial E°/\partial T)nF \qquad (10)$$

These results show that the entropy change accompanying the thermally activated electron transfer reaction (eqn. (7)) is dominated by the contribution from the cyanoferrate centre (eqn. (10)). This arises from electrostatic and specific solute-solvent interactions with the iron moiety, which are stronger in the higher charged reduced state, leading to lowering of the entropy upon reduction.[17]

Comparison of optical and electrochemical results

It follows from eqn. (1) that the temperature and pressure dependence of the MMCT energy (E_{op}) will be given by the temperature and pressure dependence of $\Delta G°$ and λ (eqns. (11) and (12)).

$$\left(\frac{\partial E_{op}}{\partial T}\right)_P = \left(\frac{\partial(\Delta G°)}{\partial T}\right)_P + \left(\frac{\partial\lambda}{\partial T}\right)_P \quad (11)$$

$$\left(\frac{\partial E_{op}}{\partial P}\right)_T = \left(\frac{\partial(\Delta G°)}{\partial P}\right)_T + \left(\frac{\partial\lambda}{\partial P}\right)_T \quad (12)$$

For symmetrical mixed valence systems, where $\Delta G°$ is necessarily zero, the temperature and pressure dependence of E_{op} will be related simply to the pressure and temperature dependence of λ. The temperature dependence of E_{op} for the symmetric complex $[(NC)_5Fe^{III}(4,4'\text{-bipyridine})Fe^{II}(CN)_5]^{5-}$ has been found to be negligible ($\partial E_{op}/\partial T = 0.1 \pm 0.6$ cm^{-1} K^{-1}).[21] In contrast to this, E_{op} for the ferri/ferrocyanide ion-pair and for a Ru^{III}–Ru^{II} dithiaspiro-bridged complex (both symmetric systems)[39,40] display significant temperature and pressure dependence ($\partial E_{op}/\partial T = 3 \pm 1$ cm^{-1} K^{-1}; $\partial E_{op}/\partial P = -1.3 \pm 0.5$ and -1.4 ± 0.2 cm^{-1} MPa^{-1}, respectively). For many previously studied asymmetrical complexes, there is a reasonable agreement between the changes in E_{op} and $\Delta E°$ induced by temperature and pressure (see Table 2), and it was concluded that the temperature and pressure dependence of λ was negligible.[21,25,26,35,41] However, in the present study, the agreement between these values is less satisfactory and the temperature and pressure dependence of λ was examined as a possible explanation for this discrepancy.

The reorganisational energy consists of intrinsic and solvent components ($\lambda = \lambda_i + \lambda_o$). A theoretical estimate of the solvent component of the reorganization energy λ_o may be obtained from eqn. (13), derived from the dielectric continuum model, where the $f(a,r)$ term is related to the size and shape of the complex and the charge transfer distance, D_{op} is the optical dielectric constant (equal to the square of the refractive index (n^2)) and D_s is static dielectric constant.

$$\lambda_o = f(a,r)\left(\frac{1}{D_{op}} - \frac{1}{D_s}\right) \quad (13)$$

There are numerous models for evaluating the function $f(a,r)$, differing in the assumptions made for the geometry of the reactants.[5,42–49] All models suffer from the problem of assigning physically-meaningful values to the radii parameters. However, regardless of which model is chosen, the $f(a,r)$ term is expected to be independent of pressure and temperature (since it is unlikely that the bond lengths will be affected by temperature or pressure in the range studied), and thus may be evaluated if λ_o is known (or calculated from eqn. (1)). The temperature and pressure dependence of λ_o can then be evaluated from eqns. (14) and (15) (which are the derivative forms of eqn. (13)), shown below.

$$\frac{\partial\lambda_o}{\partial T} = f(a,r)\left(\frac{1}{(D_{op})^2}\frac{\partial D_{op}}{\partial T} - \frac{1}{(D_s)^2}\frac{\partial D_s}{\partial T}\right) \quad (14)$$

$$\frac{\partial\lambda_o}{\partial P} = f(a,r)\times\left(\frac{1}{(D_{op})^2}\times\frac{\partial D_{op}}{\partial P} - \frac{1}{(D_s)^2}\times\frac{\partial D_s}{\partial P}\right) \quad (15)$$

As for the internal reorganisational energy, λ_i, it can be estimated by means of the harmonic oscillator model for the vibrational modes of the complex

$$\lambda_i = \sum_j \frac{f_j^r f_j^p}{f_j^r + f_j^p}(\Delta d_j)^2 \quad (16)$$

where f_i^r and f_i^p are the stretching force constants of the ith metal ligand bond in the reactant and product, respectively, and Δd_i is the change in the equilibrium bond length of the ith metal–ligand bond. The reorganisational energy will be dominated by the contribution from the cobalt centre, since it is known from crystallographic evidence that there are minimal bond length changes at the iron centre upon oxidation.[50] Molecular mechanics modelling of the mononuclear complexes[10] predicts cobalt-amine average bond length changes upon reduction of 0.16 Å for the *trans* complex and 0.18 Å for the *cis* complex. Substituting these values into eqn. (16) using the force constants 1055 kJ mol^{-1} Å^{-2} and 494 kJ mol^{-1} Å^{-2} for Co^{III}–N(amine)[51] and Co^{II}–N(amine),[52] respectively, the internal reorganisational energy is estimated to be 4300 and 5500 cm^{-1} for the *trans* and *cis* isomers, respectively. Taking into account total reorganisational energy for these systems (eqn. (1)), the solvent reorganisational energy is 5500 and 5700 cm^{-1} for the *trans* and *cis* isomers, respectively.[53] The values are very close as would be expected for complexes of similar size.

Taking the average of these values, together with the changes in D_{op} and D_s for water with temperature and pressure,[54,55] we estimate $\partial\lambda_o/\partial T$ to be 0.6 ± 0.3 cm^{-1} K^{-1}, and $\partial\lambda/\partial P$ to be -1.1 ± 0.2 cm^{-1} MPa^{-1}. Applying these values to the data for our complexes (Table 2), we find that the pressure dependent behaviour is evaluated adequately, while the temperature dependence is not. The differences can be related to changes in spin state, as explained in the following section.

Contribution of spin state

A difficulty arises when dealing with hexaaminecobalt(III/II) complexes, in that the more stable Co^{II} state is high-spin,[56] whereas the Co^{III} state is low-spin.[44,62–65] Thus, the redox potentials are related to the free energy difference between the high-spin Co^{II} and the low-spin Co^{III} states (in a three-electron process),[66] whereas the MMCT transition involves a spin-allowed one-electron transfer from Fe^{II} to Co^{III}, leading to a low-spin ($t_{2g}^6e_g^1$) electronic configuration at the cobalt centre. The $\Delta G°$ parameter relevant to eqn. (1) is then the difference between the thermally equilibrated low-spin Co^{II} and Co^{III} states, and the assumption that $\Delta G°$ can be approximated as $\Delta E°$ is no longer valid, as there is an extra term (ΔE_{isc}) involved (eqn. (17)), accounting for the energy difference between the high-spin and low-spin configurations of the cobalt(II) centre (where ΔE_{isc} is defined as $E_{(l.s.)} - E_{(h.s.)}$). This is shown qualitatively by means of a potential energy diagram in Fig. 8.

$$\Delta G° = \Delta E° + \Delta E_{isc} \quad (17)$$

In principle, ΔE_{isc} can be determined from spectroscopic data of the cobalt(II) complex.[44] However, due to the lability of the complexes in the reduced state, these data cannot be determined. However, we can at least obtain a qualitative estimate of the temperature and pressure dependence of ΔE_{isc} from studies of spin-crossover systems. It is known from many studies on the temperature and pressure dependence of spin crossover processes[67] that higher temperature favours the high-spin state, whereas higher pressure favours the low-spin state due to the energy and volume changes involved during the change in spin state. These observations would lead to a positive value of $\partial(\Delta E_{isc})/\partial T$ and a negative value of $\partial(\Delta E_{isc})/\partial P$. That is, opposite trends should be expected for the temperature and pressure dependence of the spin-state change in $\Delta G°$. If the positive $\partial(\Delta E_{isc})/\partial T$ shift is much larger than $\partial(\Delta E_{isc})/\partial P$ (as would be expected from the small contribution of pressure to inner-sphere reorganisation),[68] the differences mentioned in the previous section are easily explained.
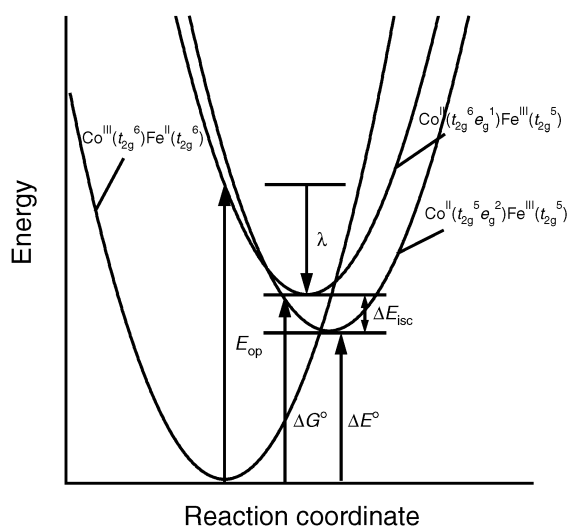
Fig. 8 Qualitative potential energy diagram of *trans-* and *cis-*[L^{14}CoNCFe(CN)$_5$]$^-$, showing the two different spin states of the Co^{II}–Fe^{III} redox isomer.

Conclusions

The redox reaction volumes obtained from pressure dependent electrochemistry in this work correlate well with earlier work on the Ru^{III}–Fe^{II} complexes [(EDTA)RuNCFe(CN)$_5$]$^{5-}$ and [(NH$_3$)$_5$RuNCFe(CN)$_5$]$^-$ and confirm the conclusions reached in that study that electrostriction is governed by the charge localised to the first coordination shell of the complex.[37] In particular, a common feature is the effective charge of 2− (Fe^{III}) and 3− (Fe^{II}) on the cyano-coordinated Fe centre, which implies that the bridging cyanide effectively donates one negative charge to the Co^{III} subunit; a result corroborated by pressure dependence of the Co$^{III/II}$ couple.

The pressure and temperature effects on the spectroscopy and electrochemistry of the complexes *trans* and *cis-*[L^{14}CoNCFe(CN)$_5$]$^-$ show that the shift in E_{op} is not fully accounted for by changes in ΔE°, and hence the pressure and temperature dependence of λ and ΔE_{isc} can not be neglected. For both isomers, the difference in the potentials of the metal centres shows a greater sensitivity to temperature and pressure than does the energy of the MMCT transition. The application of current theory to studies of dinuclear mixed valence complexes containing d^6–d^6 metal centres is complicated by the existence of multiple excited states. Evidently the high- and low-spin Co^{II} MMCT excited states are affected to different extents by temperature and pressure. We are currently looking at theoretical aspects of the MMCT process by means of DFT calculations to better understand this problem.

Acknowledgements

References

1 M. B. Robin and P. Day, *Adv. Inorg. Chem. Radiochem.*, 1967, **10**, 247–422.
2 G. C. Allen and N. S. Hush, *Prog. Inorg. Chem.*, 1967, **8**, 357–389.
3 N. S. Hush, *Prog. Inorg. Chem.*, 1967, **8**, 391–444.
4 C. Creutz, *Prog. Inorg. Chem.*, 1983, **30**, 1–73.
5 R. A. Marcus and N. Sutin, *Biochim. Biophys. Acta*, 1985, **811**, 265–322.
6 P. Chen and T. J. Meyer, *Chem. Rev.*, 1998, **98**, 1439–1477.
7 A. B. P. Lever and E. S. Dodsworth, in *Inorganic Electronic Structure and Spectroscopy*, ed. E. I. Solomon and A. B. P. Lever, Wiley, New York, 1999, vol. 2, pp. 227–287.
8 P. V. Bernhardt and M. Martínez, *Inorg. Chem.*, 1999, **38**, 424–425.
9 P. V. Bernhardt, B. P. Macpherson and M. Martínez, *Inorg. Chem.*, 2000, **39**, 5203–5208.
10 P. V. Bernhardt, B. P. Macpherson and M. Martínez, *J. Chem. Soc., Dalton Trans.*, 2002, 1435–1441.
11 P. V. Bernhardt, F. Bozoglián, B. P. Macpherson, M. Martínez, G. González and B. Sienra, *Eur. J. Inorg. Chem.*, 2003, 2512–2518.
12 P. V. Bernhardt, F. Bozoglián, B. P. Macpherson and M. Martínez, *Dalton Trans.*, 2004, 2582–2587.
13 J. I. Sachinidis, R. D. Shalders and P. A. Tregloan, *J. Electroanal. Chem.*, 1992, **327**, 219–234.
14 J. I. Sachinidis, R. D. Shalders and P. A. Tregloan, *Inorg. Chem.*, 1994, **33**, 6180–6186.
15 J. I. Sachinidis, R. D. Shalders and P. A. Tregloan, *Inorg. Chem.*, 1996, **35**, 2497–2503.
16 T. W. Swaddle and P. A. Tregloan, *Coord. Chem. Rev.*, 1999, **187**, 255–289.
17 G. I. H. Hanania, D. H. Irvine, W. A. Eaton and P. George, *J. Phys. Chem.*, 1967, **71**, 2022–2030.
18 E. L. Yee, R. J. Cave, K. L. Guyer, P. D. Tyma and M. J. Weaver, *J. Am. Chem. Soc.*, 1979, **101**, 1131–1137.
19 J. T. Hupp and M. J. Weaver, *Inorg. Chem.*, 1984, **23**, 3639–3644.
20 J. T. Hupp, G. A. Neyhart, T. J. Meyer and E. M. Kober, *J. Phys. Chem.*, 1992, **96**, 10820–10830.
21 Y. H. Dong and J. T. Hupp, *Inorg. Chem.*, 1992, **31**, 3322–3324.
22 R. van Eldik, C. Dücker-Benfer and F. Thaler, *Adv. Inorg. Chem.*, 2000, **49**, 1–58.
23 *High Pressure Chemistry: Synthetic, Mechanistic and Supercritical Applications*, ed. R. van Eldik and F.-G. Klärner, Wiley-VCH, Weinheim, 2002.
24 J. T. Hupp and Y. Dong, *J. Am. Chem. Soc.*, 1993, **115**, 6428–6429.
25 D. Chatterjee, H. C. Bajaj and A Das, *Inorg. Chem.*, 1993, **32**, 4049–4052.
26 D. E. Khoshtariya, H. C. Bajaj, P. A. Tregloan and R. van Eldik, *J. Phys. Chem. A*, 2000, **104**, 5535–5544.
27 G. A. Lawrance, T. M. Manning, M. Maeder, M. Martínez, M. A. O'Leary, W. C. Patalinghug, B. W. Skelton and A. H. White, *J. Chem. Soc., Dalton Trans.*, 1992, 1635–1641.
28 A. J. Bard and L. R. Faulkner, *Electrochemical Methods, Fundamentals and Applications*, John Wiley & Sons, New York, 2001.
29 M. Spitzer, F. Gartig and R. van Eldik, *Rev. Sci. Instrum.*, 1988, **59**, 2092–2093.
30 L. J. Farrugia, *J. Appl. Crystallogr.*, 1999, **32**, 837–838.
31 G. M. Sheldrick, *SHELX97 - Programs for Crystal Structure Analysis (Release 97-2)*, Institüt für Anorganische Chemie der Universität, Tamstrasse 4, D-3400, Göttingen, Germany, 1998.
32 L. J. Farrugia, *J. Appl. Crystallogr.*, 1997, **30**, 565.
33 A. G. Sharpe, *The Chemistry of Cyano Complexes of the Transition Metals*, Academic Press, London, 1976.
34 A. B. P. Lever, *Inorganic Electronic Spectroscopy*, Elsevier, Amsterdam, 2nd edn., 1984.
35 D. Chatterjee, H. C. Bajaj and A. Das, *Inorg. Chim. Acta*, 1994, **224**, 189–192.
36 M. Matsumoto and T. W. Swaddle, *Inorg. Chem.*, 2004, **43**, 2724–2735.
37 H. C. Bajaj, P. A. Tregloan and R. van Eldik, *Inorg. Chem.*, 2004, **43**, 1429–1435.
38 M. Martínez, M.-A. Pitarque and R. van Eldik, *Inorg. Chim. Acta*, 1997, **256**, 51–59.
39 D. E. Khoshtariya, R. Billing, M. Ackermann and R. van Eldik, *J. Chem. Soc., Faraday Trans.*, 1995, **91**, 1625–1629.
40 N. A. Lewis, Y. S. Obeng, D. V. Taveras and R. van Eldik, *J. Am. Chem. Soc.*, 1989, **111**, 924–927.
41 H. C. Bajaj and A. Das, *Polyhedron*, 1997, **16**, 3851–3855.
42 R. A. Marcus, *Annu. Rev. Phys. Chem.*, 1964, **15**, 155–196.
43 R. A. Marcus, *J. Chem. Phys.*, 1965, **43**, 679–701.
44 B. S. Brunschwig, S. Ehrenson and N. Sutin, *J. Phys. Chem.*, 1986, **90**, 3657–3668.
45 L. I. Krishtalik, *Elektrokhimiya*, 1982, **18**, 1512–1516.
46 L. I. Krishtalik, *J. Electroanal. Chem.*, 1982, **136**, 7–17.
47 P. G. Dzhavakhidze, A. A. Kornyshev and L. I. Krishtalik, *J. Electroanal. Chem.*, 1987, **228**, 329–346.
48 M. D. Newton, *Chem. Rev.*, 1991, **91**, 767–792.

49 D. E. Khoshtariya, T. D. Dolidze, L. D. Zusman, G. Lindbergh and J. Glaser, *Inorg. Chem.*, 2002, **41**, 1728–1738.
50 Estimating the internal reorganisational energy using eqn. (16) gives a value of less than 100 cm^{-1} for the iron centre.
51 P. V. Bernhardt and P. Comba, *Inorg. Chem.*, 1992, **31**, 2638–2644.
52 A. M. Bond, T. W. Hambley and M. R. Snow, *Inorg. Chem.*, 1985, **24**, 1920–1928.
53 This calculation does not take into account the difference in spin state of the cobalt centre, as discussed below. However, the errors caused by this in the estimations of λ_i, and $\Delta G°$ are somewhat compensatory. To illustrate this point, if we take the value of $\lambda_i = 1400$ cm^{-1} for [Co(sep)]$^{3+/2+}$,[44] and correct the $\Delta G°$ values of our complexes for the energy difference between the high- and low-spin states (estimated to be 3600 cm^{-1} for [Co(sep)]$^{3+/2+}$), we arrive at values of 4800 and 6200 cm^{-1} for the *trans* and *cis* isomers, respectively. The average of these values compares quite well with the average value calculated above.
54 E. M. Stanley, *J. Chem. Eng. Data*, 1971, **16**, 454–457.
55 R. C. Weast, *Handbook of Chemistry and Physics*, 51st edn., CRC Press, Cleveland, OH, 1971.
56 All known hexaaminecobalt(II) complexes have a high-spin ($t_{2g}^5 e_g^2$) electronic configuration.[57,58] Since N-bound cyanide has a similar ligand field strength to amine ligands,[59–61] the reduced *trans*- and *cis*-[L^{14}Co^{II}NCFe^{II}(CN)$_5$]$^{2-}$ complexes are also expected to be high-spin.
57 M. C. L. Yang and R. A. Palmer, *J. Am. Chem. Soc.*, 1975, **97**, 5390–5395.
58 I. I. Creaser, J. M. Harrowfield, A. J. Herlt, A. M. Sargeson, J. Springborg, R. J. Geue and M. R. Snow, *J. Am. Chem. Soc.*, 1977, **99**, 3181–3182.
59 D. F. Shriver, S. A. Shriver and S. E. Anderson, *Inorg. Chem.*, 1965, **4**, 725–730.
60 R. A. De Castello, C. P. Mac-Coll, N. B. Egen and A Haim, *Inorg. Chem.*, 1969, **8**, 699–702.
61 R. A. De Castello, C. Piriz Mac-Coll and A. Haim, *Inorg. Chem.*, 1971, **10**, 203–205.
62 A. Vogler and H. Kunkely, *Ber. Bunsen-Ges. Phys. Chem.*, 1975, **79**, 83–86.
63 H. Kunkely, V. Pawlowski and A. Vogler, *Inorg. Chim. Acta*, 1994, **225**, 327–330.
64 F. Sánchez, P. Pérez-Tejeda, F. Pérez and M. López-López, *J. Chem. Soc., Dalton Trans.*, 1999, 3035–3039.
65 M. Morillo, C. Denk, P. Pérez, M. López, A. Sánchez, R. Prado and F. Sánchez, *Coord. Chem. Rev.*, 2000, **204**, 173–198.
66 M. D. Newton, *J. Phys. Chem.*, 1991, **95**, 30–38.
67 P. Gütlich and H. A. Goodwin, in *Comprehensive Coordination Chemistry II*, ed. J. A. McCleverty and T. J. Meyer, Elsevier/Pergamon, Oxford, 2004, vol. 2, pp. 421–426.
68 J. A. Real, A. B. Gaspar, V. Niel and M. C. Muñoz, *Coord. Chem. Rev.*, 2003, **236**, 121–141.